DESY 96-053

Active Stabilization of Mechanical Quadrupole Vibrations for Linear Colliders

Christoph Montag
Deutsches Elektronen-Synchrotron DESY, D-22607 Hamburg, Germany

Submitted to *Nuclear Instruments and Methods A*

Abstract

To achieve luminosities of some $10^{33}\,\mathrm{cm}^{-2}\mathrm{s}^{-1}$, all linear collider schemes currently under study require extremely low beam emittances to achieve spot sizes of some 10 nm height and some 100 nm width at the interaction point. Therefore, high beam position stability is required in order to provide central collisions of the opposing bunches. Since ground motion amplitudes are likely to be larger than the required tolerances of 85 nm rms for the 500 GeV and 43 nm rms for the 1 TeV S-band linear collider SBLC, some means of active stabilization is necessary to damp quadrupole motion to the desired value.
Therefore, an inexpensive active stabilization system to be installed in the S-band test accelerator at DESY has been developed and successfully tested. It damps quadrupole motion in the frequency range $2 - 30$ Hz by up to 14 dB, thus leading to rms values of approximately 25 nm even in very noisy environments. Since the system is based on geophone type motion sensors with an internal noise level corresponding to 1.1 nm at 2 Hz, it is likely that this system allows stabilization below the 10 nm level.

1 Introduction

To achieve high luminosity of some $10^{33}\,\mathrm{cm}^{-2}\mathrm{s}^{-1}$, all linear collider schemes currently under study require very low emittance beams focused to spot sizes of some 10 nm vertically and some 100 nm horizontally. These tiny beam dimensions require very tight mechanical tolerances to avoid luminosity loss due to beam jitter at the interaction point caused by mechanical quadrupole vibrations. For any linac lattice with $\beta \propto \gamma^k$, $k < 0.8$, and constant phase advance μ per FODO cell, the maximum tolerable uncorrelated quadrupole jitter σ_q leading to a luminosity degradation of 3% due to beam offset at the IP can be estimated as [1, 2]

$$\sigma_\mathrm{q} = 0.25 \cdot \sqrt{\frac{\epsilon_\mathrm{end} \cdot \overline{\beta}_\mathrm{end}}{N_\mathrm{q}}} \cdot \cos\frac{\mu}{2} \tag{1}$$

$$= 0.25 \cdot \overline{\beta}_\mathrm{end} \cdot \sqrt{\frac{\epsilon_\mathrm{end} \cdot (1-k) \cdot \sin\mu}{2 \cdot L}} \cdot \cos\frac{\mu}{2}, \tag{2}$$

where ϵ_end, $\overline{\beta}_\mathrm{end}$, N_q are the geometric emittance at the end of the linac, the average β-function of the last FODO cell, and the total number of quadrupoles in the linac, respectively. L is the total linac length.
Using the parameters given in table 1, one gets a vertical tolerance level of 85 nm for the 500 GeV and 43 nm for the 1 TeV S-band linear collider SBLC [3], while in the horizontal plane these numbers relax to 380 nm and 430 nm, respectively. In the final focus system, these tolerances

are even tighter by a factor of about 5 to 10, but they cannot be expressed by eq. (1) [4, 5]. Since ground motion measurements (fig. 1) at DESY [6] indicate that vertical vibration tolerances are exceeded in an active accelerator environment at frequencies higher than those the beam based feedback systems are capable to compensate, one has to invent direct vibration measurement and compensation techniques. Due to the large number of quadrupoles in the main linac, the costs of each system should not exceed a limit of about 10000 \$, while much more effort can be spent in the final focus with its much smaller tolerances. Therefore, an inexpensive active mechanical stabilization system based on geophones as vibration sensors and piezoelectric actuators to decouple the linac magnets from ground motion has been developed. Aim of these investigations was to demonstrate active quadrupole stabilization in a typical accelerator environment.
This paper describes the considerations that led to the present design of the system as well as the system itself.

2 Support philosophy

For compensation purposes, the ground motion spectrum can be splitted up into various frequency domains, each of them requiring different compensation schemes [7].
As the experience at SLAC has shown, beam-based orbit correction schemes can be successfully employed only in the low frequency region where $f < f_{\mathrm{rep}}/25$ [8]. Above this frequency limit, the compensation capability of any beam-based method is not sufficient, and even leads to an amplification of the beam jitter amplitudes for higher frequencies. To overcome this limitation, the linear collider quadrupole vibrations have to be either compensated passively or measured independently of the beam and compensated by some means in order to fight beam jitter at its source.
The simplest passive damping system consists of some kind of "spring" with a resonance frequency f_r and damping constant δ acting as magnet support, which leads to an attenuation of vibration amplitudes at frequencies well above this resonance frequency proportional to $1/\omega^2$ according to the transfer function

$$H_r(s) = \frac{\omega_r^2}{s^2 + 2\delta\omega_r s + \omega_r^2} \tag{3}$$

of a passive vibration absorber. Here, $s = i\omega$ is the Laplace variable, while $\omega_r = 2\pi f_r$.
Since in the case of the SBLC with a repetition rate f_{rep} of 50 Hz the limiting frequency for beam based orbit correction schemes is some 2 Hz, it would be necessary to build a passive quadrupole support with a resonance frequency f_r of approximately 1 Hz to achieve an attenuation by a factor of 5 at 2 Hz. If one assumes a magnet weight of 100 kg, this corresponds to a spring constant D of $4000\,\mathrm{N}\cdot\mathrm{m}^{-1}$.
Though such a system would be capable to damp ground motion to the desired value due to its small transmissibility, it would nevertheless be very sensitive to any force acting on the magnet itself (high compliance). For example, a static force as small as $4\cdot10^{-3}$N would lead to a static magnet displacement of 1μm. In the frequency domain, the resulting amplitude $A(s)$ per unit force $F(s)$ as function of the Laplace variable s can be written as

$$A(s) = \frac{\frac{\omega_r^2}{D}}{s^2 + 2\delta\omega_r s + \omega_r^2} \cdot F(s) \tag{4}$$

$$= H_r(s) \cdot \frac{F(s)}{D} \tag{5}$$

$$= H_r(s) \cdot \frac{F(s)}{\omega_r^2 \cdot m}. \tag{6}$$

D is the spring constant and δ the damping constant of the magnet support "spring".
Using $s = i\omega$, figure 2 shows the modulus of this transfer function for forces acting on the magnet itself and resulting in vibration amplitudes, like for example coil vibrations due to cooling water pressure fluctuations, for three different resonance frequencies $f_r = 1\,\mathrm{Hz}$, $10\,\mathrm{Hz}$ and $100\,\mathrm{Hz}$.
These considerations led to the development of an active stabilization system with a vibration sensor on top of each magnet and some means of actuator to move the magnet in order to keep it at rest.
At this point, again a decision has to be made about the mechanical resonance frequency of the active support. One might think of an intermediate frequency of about $f_r = 10\,\mathrm{Hz}$, which would lead to an attenuation of higher frequencies just due to its passive mechanical behaviour, while slow vibrations have to be compensated actively using for example an electrodynamic transducer. Assuming a motion sensor with a lower frequency limit f_s and transfer function H_s, together with the transfer function H_r of the support

$$H_r = \frac{\omega_r^2}{s^2 + 2\delta\omega_r s + \omega_r^2} \tag{7}$$

and a feedback algorithm F, one gets the transfer function

$$H_g = \frac{H_r}{1 + F H_r H_s}, \tag{8}$$

which describes the transfer of ground motion amplitudes to the magnet. On the other hand, the transfer function for exciting forces acting on the magnet directly becomes

$$H_m = \frac{\frac{1}{D}}{1 + F H_r H_s}. \tag{9}$$

Since $\lim_{s\to 0} H_s(s) = 0$ due to the finite lower frequency limit f_s and $\lim_{s\to\infty} H_r(s) = 0$ (eq. (7)),

$$\lim_{s\to 0} H_m(s) = \lim_{s\to\infty} H_m(s) = \frac{1}{D}, \tag{10}$$

the effective spring constant H_m^{-1} in the limit of low and high frequencies equals the passive spring constant D of the magnet support. Therefore, the mechanical resonance frequency and correspondingly the spring constant of the support are chosen as high as possible.

3 Vibration sensors

The noise of geophone type vibration sensors measuring the velocity of ground motion has been determined to ensure their applicability in the active stabilization system [9].
This is not trivial because it is very difficult to provide a perfectly quiet environment as a noise-free reference. Instead, two sensors of the same type have been placed side-by-side, so both of them measured the same ground motion signal, as schematically shown in figure 3

[10]. The output signals $x(t)$ and $y(t)$ of both sensors with transfer functions H_1 and H_2 where simultaneously sampled and digitized at 1 kHz. As indicated in fig. 3, these output signals consist of the input signal $u(t)$, transferred to the corresponding sensor, and a certain amount of noise $n_1(t)$ and $n_2(t)$, respectively.
Using the Laplace transformation, these relations can be written as

$$X(s) = H_1(s) \cdot U(s) + N_1(s) \tag{11}$$
$$Y(s) = H_2(s) \cdot U(s) + N_2(s), \tag{12}$$

where $X(s)$ is the Laplace transform of $x(t)$, etc.
Resolving eq. (11) for $U(s)$ and inserting this into equation (12), this yields

$$Y(s) = H(s) \cdot X(s) + N(s), \tag{13}$$

with

$$H(s) = \frac{H_2(s)}{H_1(s)}, \tag{14}$$
$$N(s) = N_2(s) - H(s) \cdot N_1(s). \tag{15}$$

The corresponding scheme is shown in figure 4.
From the two output signals $x(t)$ and $y(t)$, the power spectrum density of both the ground motion and the internal noise of the sensors can be obtained using the correlation function [11]

$$\gamma = \frac{\Phi_{xy}}{\sqrt{\Phi_{xx}\Phi_{yy}}}, \tag{16}$$

with

$$\Phi_{xx} = \overline{X(\omega)X^*(\omega)}, \tag{17}$$
$$\Phi_{yy} = \overline{Y(\omega)Y^*(\omega)}, \tag{18}$$
$$\Phi_{xy} = \overline{X(\omega)Y^*(\omega)}, \tag{19}$$

where $X(\omega)$ is the Fourier transform of $x(t)$, etc.
The averaged power spectra Φ have been calculated dividing each time series into overlapping segments, the overlap being 62.5% [12], and Fourier-transforming these segments using a Hanning window.
Utilizing the power spectra Φ_{xx}, Φ_{yy} and Φ_{xy}, one gets the following relations:

$$H = \frac{\Phi_{xy}}{\Phi_{xx}}, \tag{20}$$
$$\Phi_{nn} = \Phi_{yy} - |H|^2\Phi_{xx}, \tag{21}$$
$$\Phi_{ss} = \Phi_{yy} \cdot |\gamma|^2, \tag{22}$$
$$\beta = \frac{\Phi_{xx}|H|^2}{\Phi_{nn}} \tag{23}$$
$$= \frac{|\gamma|^2}{1-|\gamma|^2}, \tag{24}$$

where Φ_{nn}, Φ_{ss}, β are the noise power spectrum, signal power spectrum, and the signal-to-noise ratio, respectively.

This method has been applied to geophone type motion sensors manufactured by KEBE Scientific Instruments having a transfer function shown in figure 5.
The rms value σ_n in a certain frequency band f_0 to f_1 can be calculated by integrating the noise power spectrum Φ_{nn} over this frequency band:

$$\sigma_n^2 = \int_{\omega_0=2\pi f_0}^{\omega_1=2\pi f_1} \Phi_{nn}(\omega) d\omega. \tag{25}$$

Figure 6 shows the rms noise level of the KEBE sensors in the frequency band f_0 to infinity as function of the lower frequency f_0 :

$$\sigma_n(f > f_0) = \sqrt{\int_{\omega_0=2\pi f_0}^{\infty} \Phi_{nn}(\omega) d\omega} \tag{26}$$

The resulting rms noise level in the frequency band from 2 Hz to infinity has been determined at 1.1 ± 0.3 nm, which is well below the quadrupole jitter tolerance even for the 1 TeV machine. Therefore, these sensors have been considered useful for the active stabilization system.

4 Design of the active stabilization system

For simplicity reasons as well as cost limitation, the mechanical design is based on a single piezoelectric actuator tilting the quadrupole around its transverse horizontal axis thus keeping its center at rest, as schematically shown in figure 7. As can be easily shown, the magnet optics effect of this tilt can be neglected compared to the corresponding offset of its center.
The opposite end of the magnet is placed on two massive ball-ended feet to reduce dry friction. To fix the magnet's horizontal position, two horizontal "arms" with sufficient vertical compliance but high stiffness in the horizontal directions have been placed on one side of the quadrupole. The KEBE sensor is mounted on top of the magnet just above its center.
The lowest mechanical resonance frequency of this support has been measured to be $f_r = 143$ Hz, which, together with the magnet mass of approximately 100 kg, corresponds to a spring constant D of about 80 Nμm^{-1}.
The whole system is placed on a very stiff concrete support with high internal damping to avoid amplification of ground motion due to mechanical resonances. As experimentally confirmed, it has no mechanical eigenmodes in the frequency range up to 300 Hz. The triangular cross section ensures the transfer of horizontal ground motion without amplification.
The complete active quadrupole support is shown in figure 8.
For this first prototype of the active stabilization system, the feedback circuit has been realized on a PC with 16 bit A/D board. The algorithm consists of a 100 sec highpass filter to cut offsets of the input signal, an integrator to get the displacement from the velocity signal, and several digital filters, as schematically shown in fig. 9.

5 Results of active stabilization

The active stabilization system has been set up in DESY hall 2, an experimental hall close to the DESY synchrotrons which has been chosen for the installation of the S-band test linac. Since there are two accelerators, several transformers and some other technical equipment operated nearby, it is considered as a typical example of an operating Linear Collider environment. Therefore, the results obtained in this place should be comparable to those to be expected in

the future accelerator.
To determine the performance of the system, a second KEBE sensor was placed on the floor just below the magnet. The signals of the feedback sensor as well as this second one where simultaneously sampled at 400 Hz to exclude artefacts in the results due to the statistical behaviour of ground motion. Sets of 1024 data points each were integrated to obtain the displacement from the velocity signal, multiplied by a Hanning window and Fourier-transformed in order to determine the power spectra Φ_{xx} and Φ_{yy} of the two signals. From these power spectra, the rms values σ_x and σ_y of the displacement in the frequency band f_0 to infinity can be calculated as

$$\sigma(f > f_0) = \sqrt{\int_{\omega_0=2\pi f_0}^{\infty} \Phi(\omega) d\omega}. \tag{27}$$

To ensure the reliability of this method, signals of both sensors where processed with the feedback system switched off. In this case, the transfer function is expected to be unity. As shown in figure 10, this is indeed the case in the frequency region below approximately 30 Hz, while amplitudes of vibrations beyond this limit appear to be higher on top of the magnet than on the floor. This latter effect results from the lowest mechanical resonance at 143 Hz, but due to the small ground motion amplitudes in this frequency region its contribution to the rms value is negligible. With the feedback switched on, this effect is slightly amplified (fig. 11) but still does not appear to be harmful. Below 30 Hz, the damping effect is clearly visible.
The measured feedback gain calculated as the square root of the ratio of the two power spectra is shown in figure 12, together with the theoretically expected curve.
As already mentioned in the introduction, the aim of active stabilization was to reduce the (uncorrelated) quadrupole jitter to an rms value of less than 43 nm for the 1 TeV S-band linear collider. Fig. 13 presents the rms value σ of simultaneously measured ground and magnet motion as a function of the lower cut-off frequency f_0, as has been calculated from the power spectra shown in fig. 11. Although a vertical ground motion rms value of 100 nm at $f_0 = 2$ Hz is considered a noisy environment, the active stabilization system is capable to damp magnet motion to an rms value of about 26 nm in this frequency band. Taking into account the very low internal noise of the sensors, one can expect even lower values in less noisy environments.
To investigate the influence of cooling water pressure fluctuations known as a main source of high frequency quadrupole vibrations for example at SLAC [14], magnet motion power spectra have been obtained with cooling water switched on and off. While the design water flow is 120 l/h, these data were taken at an increased flow of 220 l/h. It turned out that the influence of cooling water is almost negligible. The only difference in both power spectra is a small enhancement around 100 Hz which practically does not contribute to the magnet motion rms value.
Nevertheless, all data presented in figs. 11 to 13 were obtained at a cooling water flow of 220 l/h.

6 Conclusion

As has been experimentally demonstrated, active stabilization of mechanical quadrupole vibrations is possible down to approximately 25 nm for vibration frequencies higher than 2 Hz even in quite noisy environments with ground motion amplitudes of 100 nm in the same frequency range. In less noisy places, an rms value of less than 10 nm is likely to be achieved due to the very low noise level of the motion sensors. Therefore, the system presented in this paper might be even applicable in the final focus system of the S-band linear collider SBLC, provided that

the final focus is located in a less noisy environment.
At present time, the complete active stabilization system costs approximately 10000 $, which will surely reduce for a large number of systems.
Though the required tolerances might be achievable even without any active stabilization, a retrofit of the machine with the system described in this paper can be considered as a luminosity upgrade option.
Compared to any correction scheme based on dipole correctors to compensate magnet motion detected by a geophone, a mechanical system has two advantages. First of all, the unexpensive sensors used in the system presented in this paper would not be applicable because of the large range in the phase shift of their transfer function. Therefore, more sophisticated motion sensors have to be used, usually being more expensive.
Secondly, the performance of the presented system can be monitored online by taking data from the geophones on top of each quadrupole.

7 Acknowledgements

The author wants to thank J. Rossbach, R. Brinkmann, N. Holtkamp and G. A. Voss for many valuable and stimulating discussions and G. Meyer and H. Kaiser for the excellent mechanical design of the magnet support.

References

[1] T. O. Raubenheimer, The Generation and Acceleration of Low Emittance Flat Beams for Future Linear Colliders, SLAC report 387, 1991

[2] J. Rossbach, Tolerance on Uncorrelated Motion of Quadrupoles for Linear Colliders, DESY M/VM 93-01

[3] N. Holtkamp et al., Status of the S-Band Linear Collider Study, DESY M-93-05

[4] K. Oide, Final Focus System for the JLC, KEK Preprint 89-190

[5] O. Napoly, CLIC Final Focus System: Upgraded Version with Increased Bandwidth and Error Analysis, CEA/DAPNIA/SEA 94 10

[6] V. Shiltsev, B. Baklakov, P. Lebedev, C. Montag, J. Rossbach, Measurements of Ground Vibrations and Orbit Motion at HERA, DESY HERA 95-06

[7] C. Montag, J. Rossbach, A Mechanical Feedback System for Linear Colliders to Compensate Fast Magnet Motion, Proc. PAC 95

[8] M. G. Minty, C. Adolphsen, L. J. Hendrickson, R. Sass, T. Slaton, M. Woodley, Feedback Performance at the Stanford Linear Collider, SLAC Preprint; see also M. Ross, SLC Linac Vibration Study, Sixth International Workshop on Linear Colliders LC 95, KEK Proceedings 95-5

[9] C. Montag, M. Lomperski, J. Rossbach, Studies of Measurement and Compensation Techniques of Magnet Motion for Linear Colliders, Proc. EPAC 94

[10] S. D. Stearns, Applications of the Coherence Function in Comparing Seismometers, preprint, Albuquerque 1979

[11] S. D. Stearns, Digital Signal Analysis, Hayden, 1975

[12] G. C. Carter et al., Estimation of the Magnitude-Squared Coherence Function via Overlapped Fast Fourier Transform Processing, IEEE Trans. Au-21, No. 4, August 1973

[13] Dr. Kebe Scientific Instruments GmbH, Schwingungsmesser SMK-1, manual, Halstenbek 1994

[14] J. L. Turner and R. Stege, Vibration of Linac Quadrupoles at 59 Hz, SLAC Collider Note 399

List of Figures

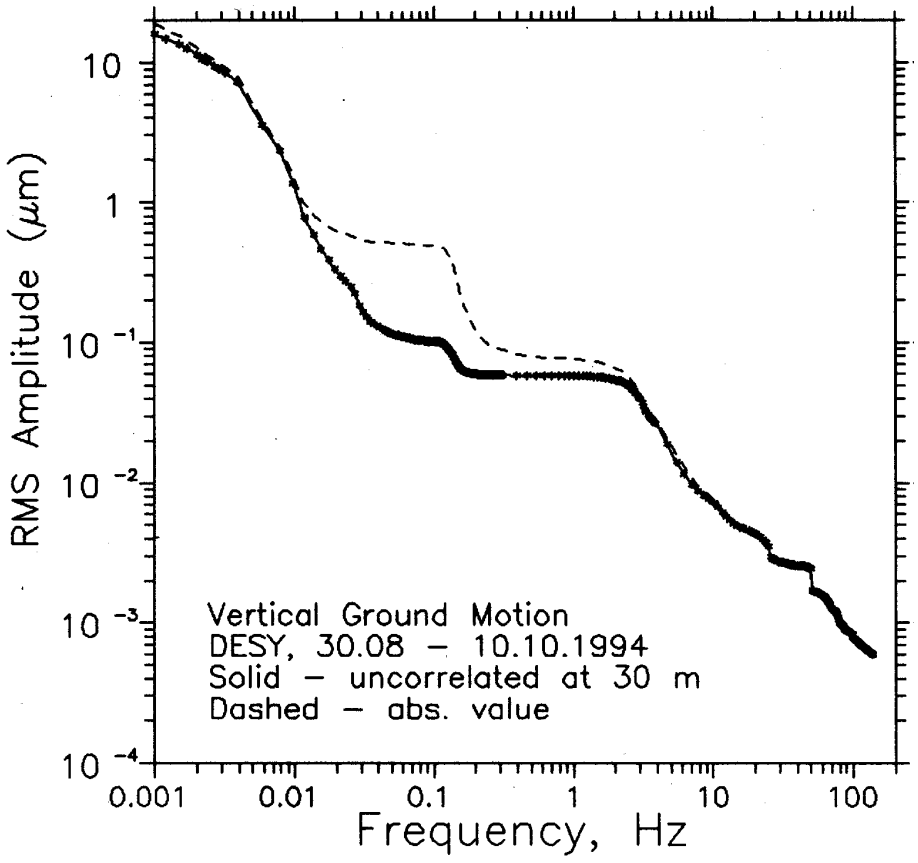

Figure 1: rms values of ground motion measured in HERA Hall West.

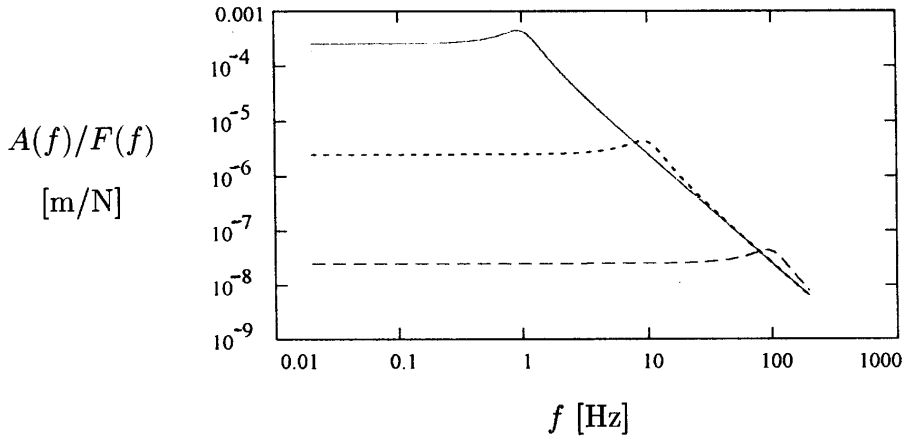

Figure 2: Transfer function for forces $F(f)$ acting on the magnet itself and resulting in displacement $A(f)$ according to equation (4) with $m = 100\,\mathrm{kg}$ and $\delta = 0.3$ for three different resonance frequencies $f_r = 1\,\mathrm{Hz}$, $10\,\mathrm{Hz}$ and $100\,\mathrm{Hz}$.

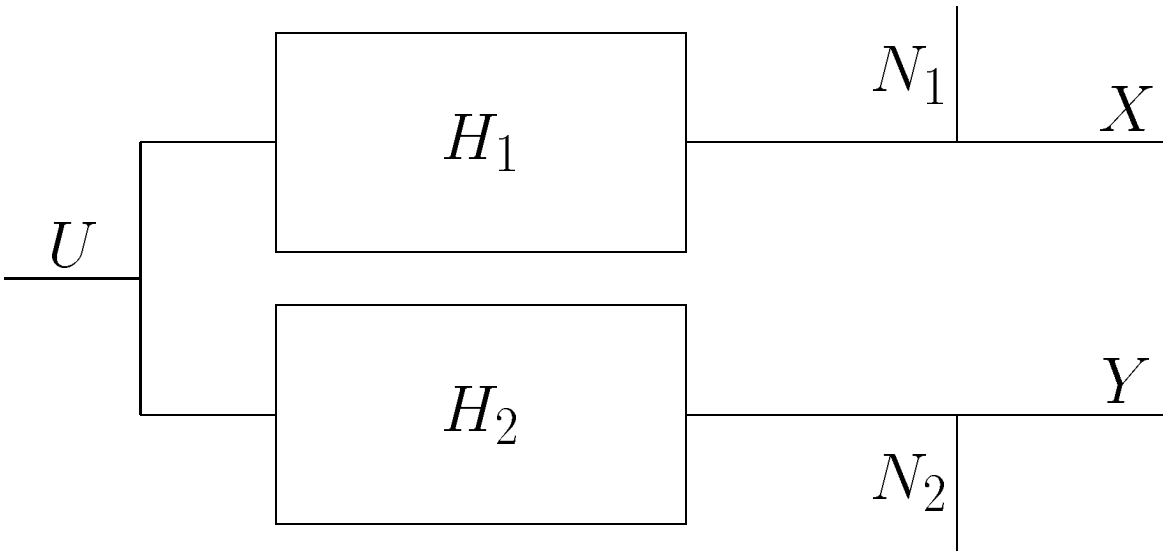

Figure 3: Schematic view of two sensors measuring the same input vibration.

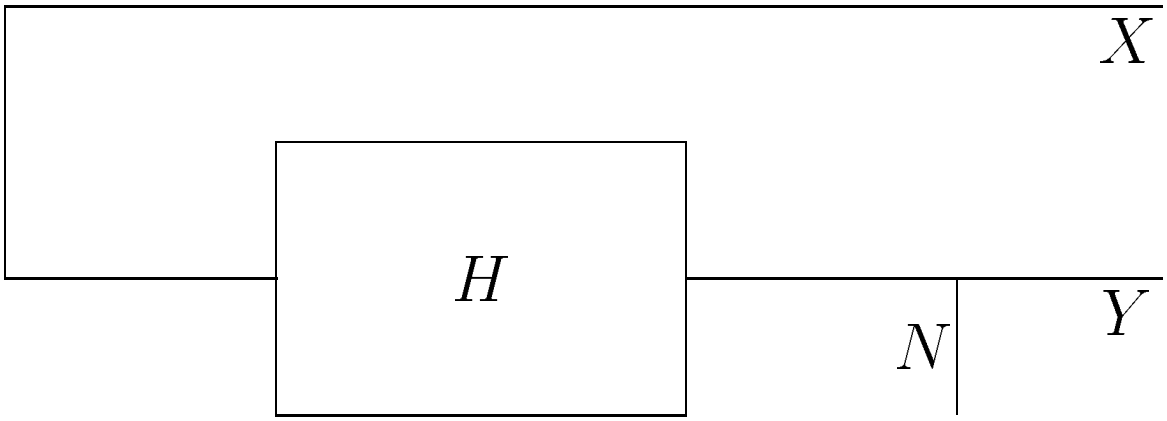

Figure 4: Equivalent scheme for coherence study.

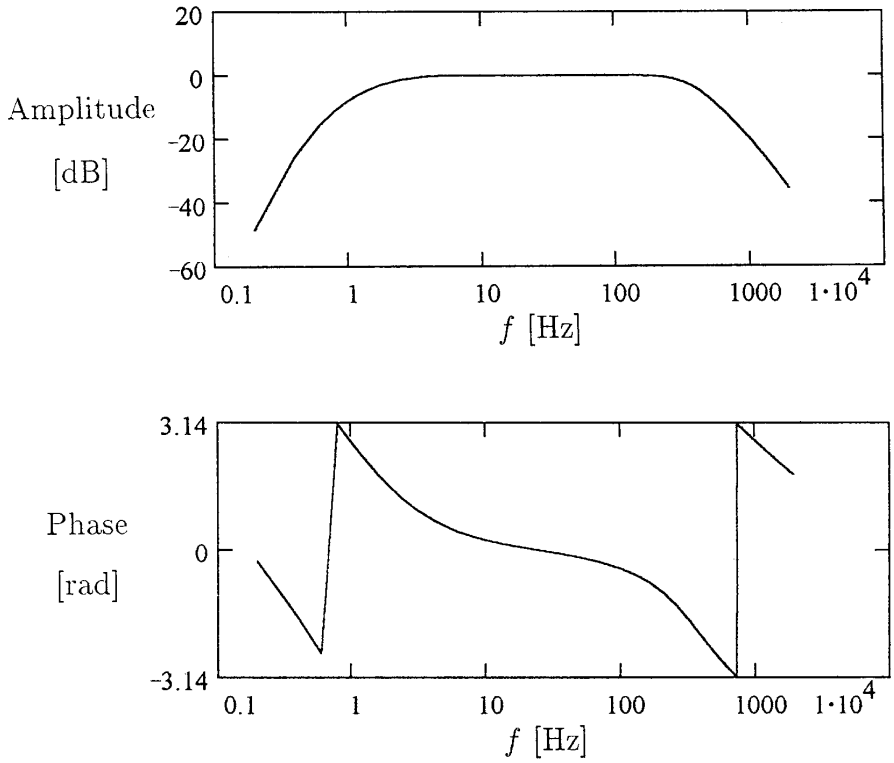

Figure 5: Bode plot of the KEBE geophone with preamplifier. The amplitude is normalized to 0 dB at 16 Hz.

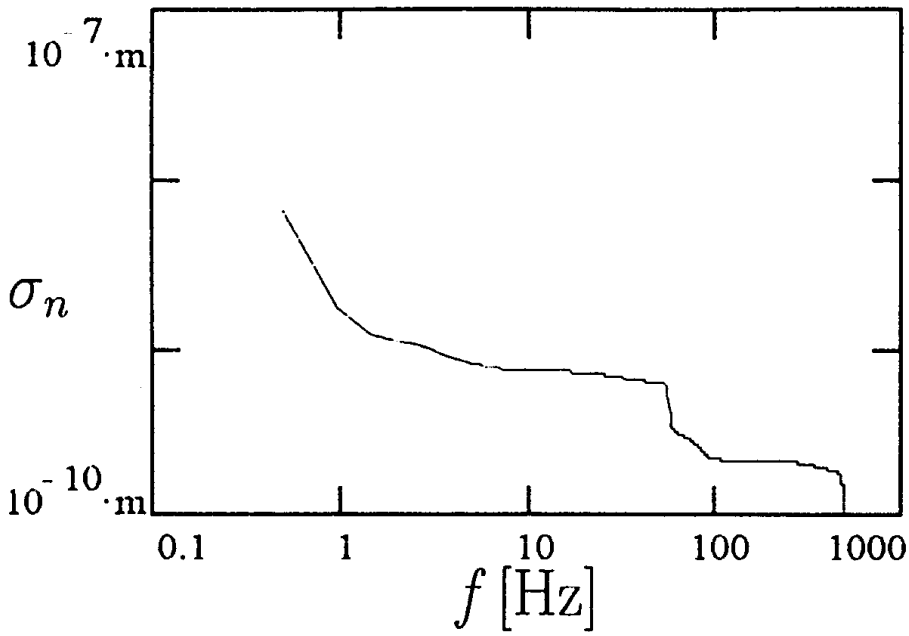

Figure 6: rms value of the internal noise of the KEBE sensors in the frequency band f_0 to infinity as function of the lower frequency f_0.

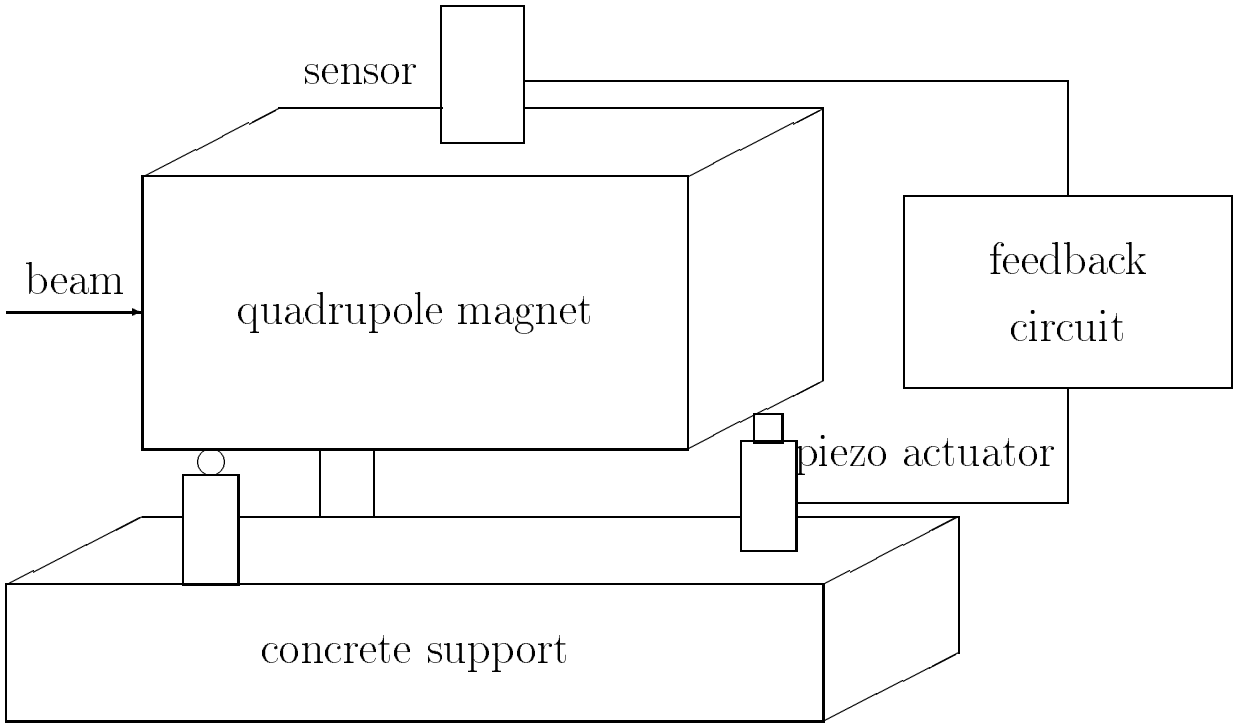

Figure 7: Schematic view of the active stabilization system.

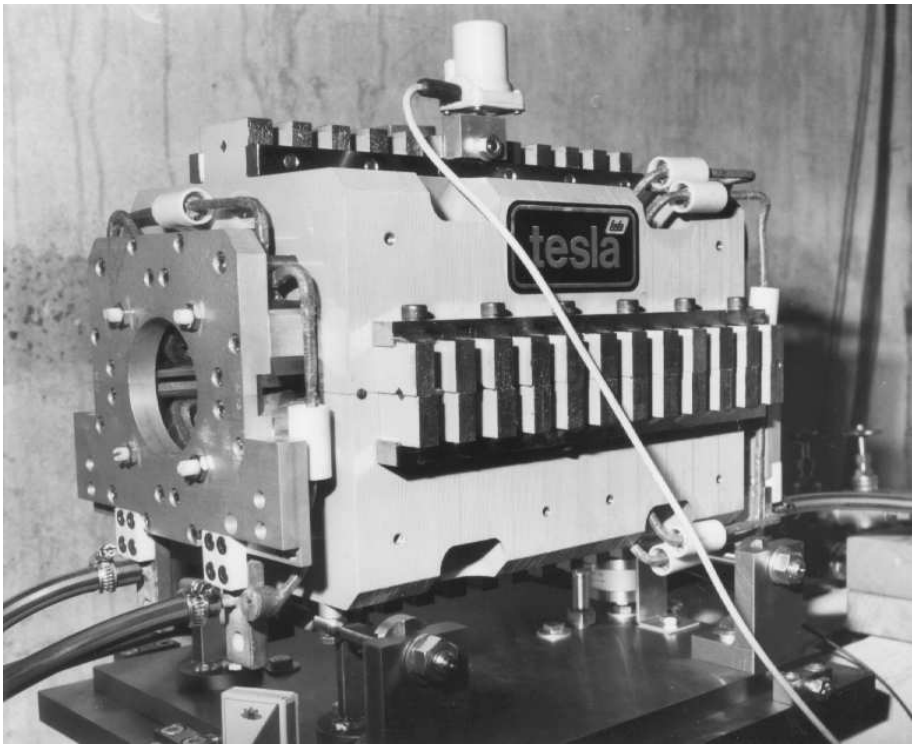

Figure 8: Active stabilization system, consisting of a KEBE geophone on top of the magnet and a piezo actuator below it to tilt the quadrupole around its horizontal transverse axis. A match-box in the front indicates the size.

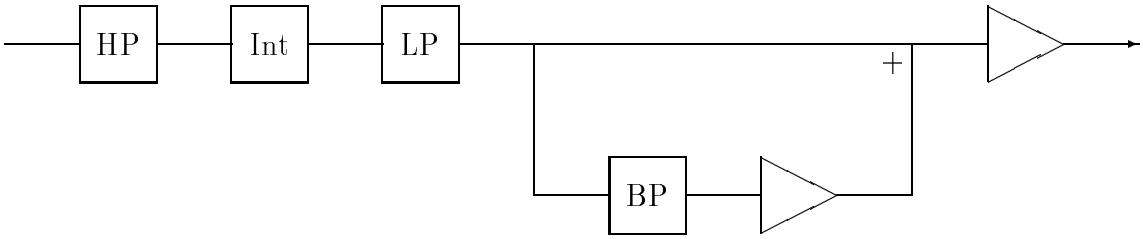

Figure 9: Schematic view of the feedback algorithm, consisting of an integrator (Int) and several digital filters (lowpass LP, highpass HP, bandpass BP).

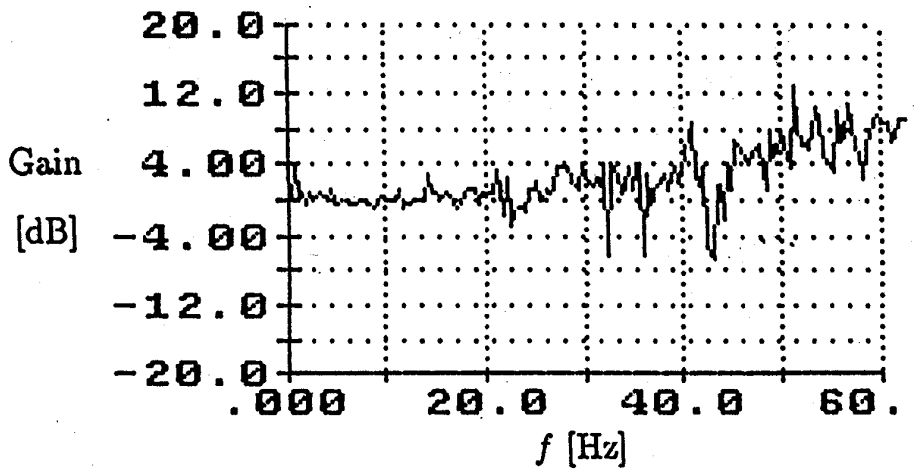

Figure 10: Measured transfer function for ground motion acting on the magnet with the feedback system switched off.

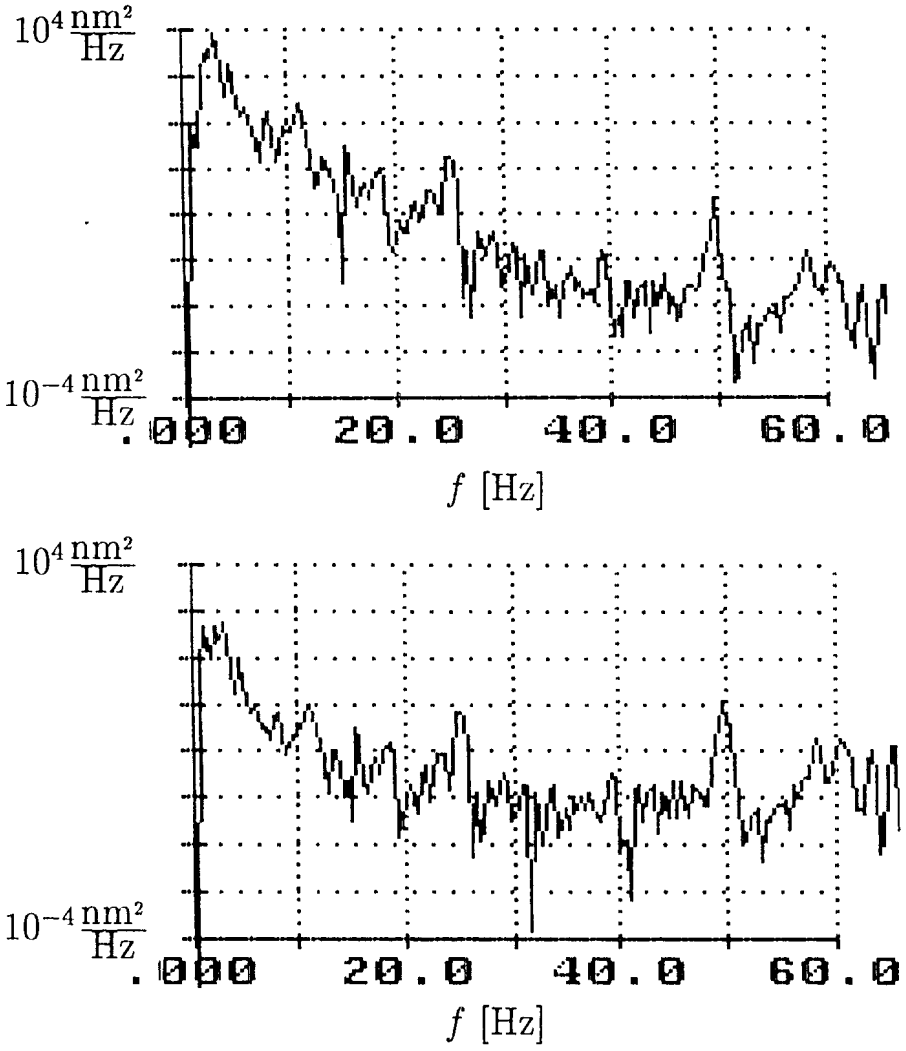

Figure 11: Simultaneously measured power spectra of ground (top) and magnet motion (bottom) with the feedback system switched on.

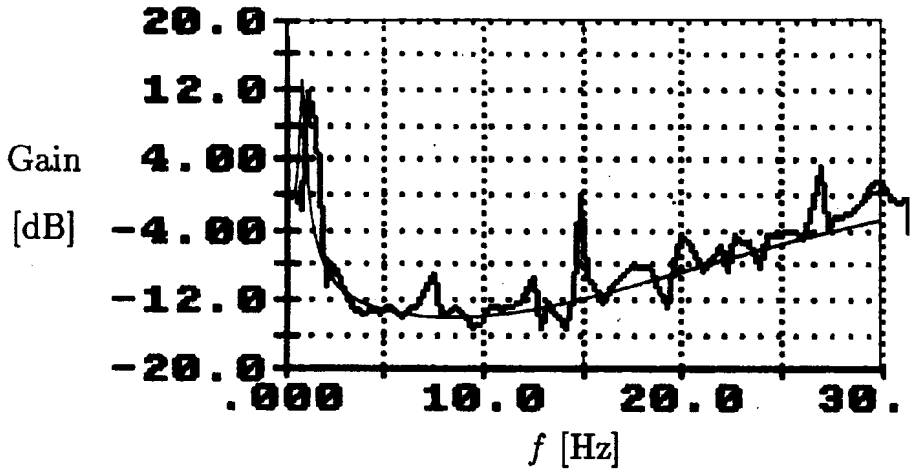

Figure 12: Measured feedback gain (thick line) in the frequency band from 0 to 30 Hz, calculated from the square root of the ratio of the two power spectra shown in figure 11. The smooth thinner curve shows the theoretical transfer function.

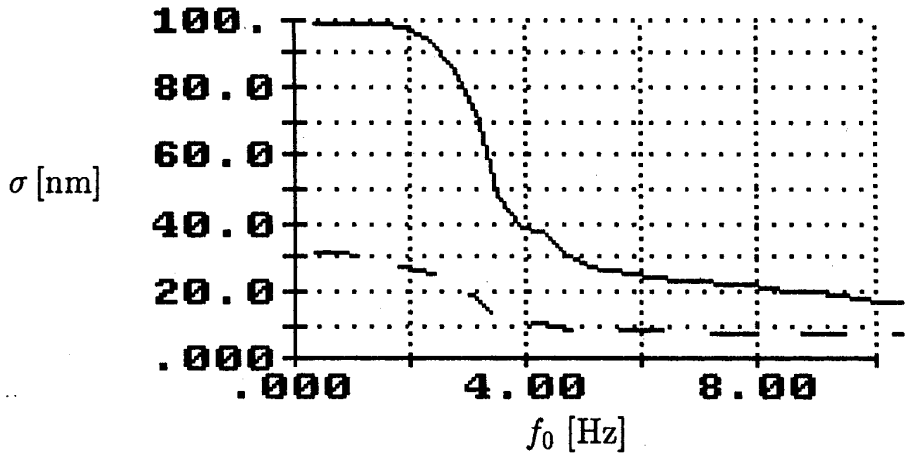

Figure 13: rms value of ground (solid) and magnet motion (dashed) with the feedback system switched on in the frequency band f_0 to infinity as function of the lower frequency f_0, f_0 ranging from 0 to 10 Hz.

List of Tables

	SBLC	
$E\,[\mathrm{GeV}]$	500	1000
$\overline{\beta}_{\mathrm{v,end}}\,[\mathrm{m}]$	165	233
$\overline{\beta}_{\mathrm{h,end}}\,[\mathrm{m}]$	165	233
$\gamma \cdot \epsilon_{\mathrm{v,end}}\,[\mathrm{m} \cdot \mathrm{rad}]$	$2.5 \cdot 10^{-7}$	$0.5 \cdot 10^{-7}$
$\gamma \cdot \epsilon_{\mathrm{h,end}}\,[\mathrm{m} \cdot \mathrm{rad}]$	$5 \cdot 10^{-6}$	$5 \cdot 10^{-6}$
k	0.5	0.5
μ	$\pi/2$	$\pi/2\sqrt{2}$
$2 \cdot L\,[\mathrm{km}]$	29.4	29.4

Table 1: Parameters of the S-band linear collider SBLC relevant for the estimation of quadrupole jitter tolerances.